

## Structural Rearrangements in Water Viewed Through Two-Dimensional Infrared Spectroscopy

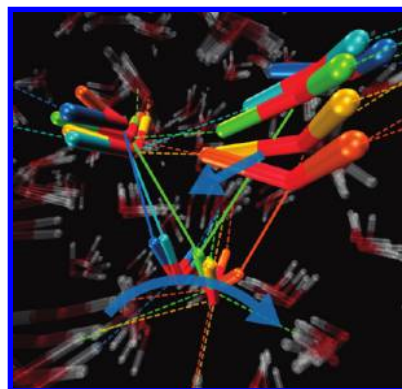
SEAN T. ROBERTS, KRUPA RAMASESHA, AND  
ANDREI TOKMAKOFF\*

*Department of Chemistry, Massachusetts Institute of Technology,  
Cambridge, Massachusetts 02139*

RECEIVED ON MARCH 17, 2009

### CON SPECTUS

Compared with other molecular liquids, water is highly structured because of its ability to form up to four hydrogen bonds, resulting in a tetrahedral network of molecules. However, this underlying intermolecular structure is constantly in motion, exhibiting large fluctuations and reorganizations on time scales from femtoseconds to picoseconds. These motions allow water to play a key role in a number of chemical and biological processes. By exploiting the fact that the OH stretching frequency of dilute HOD in liquid D<sub>2</sub>O is highly dependent upon the configuration of the neighbor nearest to the proton, researchers have been able to track water's time-dependent structure using two-dimensional infrared (2D IR) spectroscopy, which tags molecules at an initial frequency and then watches as that frequency evolves with respect to time. Recent advances in molecular dynamics simulation techniques allow for the calculation of 2D IR spectra, providing an atomistic interpretation tool of 2D IR spectra in terms of the underlying dynamics of the liquid. In this Account, we review recent ultrafast 2D IR studies at MIT that provide new information on the mechanism of hydrogen-bond rearrangements in liquid water.



The 2D IR spectra of the OH stretching vibration of HOD in D<sub>2</sub>O appear highly asymmetric. In the frequency range indicative of hydrogen-bonded molecules (<3300 cm<sup>-1</sup>), the 2D spectra remain fairly compact. By contrast, in the frequency range in which molecules having weak or broken hydrogen bonds absorb (>3500 cm<sup>-1</sup>), the 2D spectra broaden over a time scale of ~60 fs, consistent with librations (hindered rotations) of water molecules. This broadening indicates that molecules forming weak or broken hydrogen bonds are unstable and reorient rapidly to return to a hydrogen-bonded configuration.

These conclusions are supported by the results of molecular dynamics simulations, which suggest that water molecules undergo a large-angle reorientation during the course of hydrogen-bond exchange. The transition state for hydrogen-bond rearrangements is found to resemble a bifurcated hydrogen bond. Roughly half of the hydrogen-bond exchange events in the simulation are found to involve the insertion of a water molecule across a hydrogen bond, suggesting that hydrogen-bond exchange in water involves the correlated motion of water molecules as far away as the second solvation shell.

The combination of ultrafast 2D IR spectroscopy with simulation-based modeling is leading to self-consistent descriptions of the underlying dynamics in liquid water. Moreover, these results also demonstrate a more general, unique characteristic of the spectroscopy: if a spectral signature of the transition state exists, then 2D IR can effectively serve as a transition-state spectroscopy.

### Introduction

Although it is key to many chemical and biological processes, a molecular understanding of how the structure of liquid water evolves with time continues to challenge researchers. While the structure of most liquids is dominated by repulsive

forces, the additional attractive hydrogen-bonding interactions in water lead to its unique properties. The ability of water to accept and donate two hydrogen bonds gives rise to a constantly evolving disordered tetrahedral network of molecules. At any instant, liquid water contains ~90%

of the hydrogen bonds formed in ice.<sup>1,2</sup> Yet, the weak nature of hydrogen bonds allows the connectivity of water's network to rapidly fluctuate and rearrange over time scales from tens of femtoseconds to picoseconds.<sup>3–5</sup> Such structural fluctuations combined with the water molecule's large dipole moment form the heart of aqueous reactivity, allowing water to rapidly respond to changes in solute electronic structure<sup>6</sup> and guide the motion of protons through solution.<sup>7</sup>

Numerous conceptual descriptions of liquid water's structure have been put forth based on decades of experiments, theory, and computer simulations. It is common to discuss hydrogen bonding in water from the perspective of instantaneous structure and the variation of hydrogen bond configurations. Broadly speaking, such proposals fall into two types of categories:<sup>1</sup> (1) continuum models, which argue that water is composed of a continuous distribution of hydrogen-bonded configurations, or (2) mixture models, which instead posit that water is comprised of two or more distinct hydrogen-bonding species. Structural perspectives on water that ignore the ultrafast hydrogen bond dynamics neglect the fact that there are also small barriers between configurations and rapid changes in hydrogen bond connectivity that are equally important to understanding water's physical and chemical properties. An alternate perspective that we take here is that questions about the nature of water structure can be discussed in terms of dynamics. Specifically, what is the mechanism by which hydrogen bonds in water rearrange? Regardless of the approach, all studies of water share a common barrier to developing a broadly accepted view of the liquid: There is no unique definition of a hydrogen bond.

Until recently, experiments that directly characterize changes in water's structure over the relevant femtosecond time scales have been lacking. X-ray and neutron scattering measure average structural properties over molecular length scales, but these experiments are not time-resolved.<sup>2,8</sup> Dielectric relaxation and nuclear magnetic resonance dipolar relaxation can be modeled to provide an average reorientation time scale for water molecules, but they are not structurally sensitive and also do not directly observe these molecular motions.<sup>9</sup> Femtosecond solvation dynamics experiments<sup>6,10</sup> and optical Kerr effect measurements<sup>3,11,12</sup> have femtosecond time resolution but lack sensitivity to water's hydrogen bond structure.

From a computational perspective, classical molecular dynamics (MD) simulations have allowed researchers to test proposals for water's structure in microscopic detail. Simulations clarify the types of orientational and translational fluctuations that water molecules undergo within a stable local

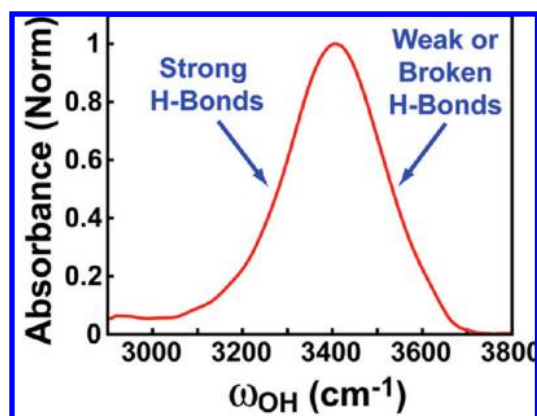


FIGURE 1. Infrared absorption spectrum of  $\sim 1\%$  HOD in  $D_2O$ .

configuration on femtosecond time scales and reveal the loosely correlated motion of many molecules involved in picosecond hydrogen bond rearrangements.<sup>5,13,14</sup> However, MD simulations are based on models often parametrized to reproduce bulk thermodynamic properties, and it is not clear whether their predictions for microscopic fluctuations are accurate. Simulations need to be compared with experimental benchmarks to prove their validity for dynamics.

Time-resolved infrared spectroscopy has the ability to fill the missing gap between experiments and simulation since water's O–H stretching frequency is sensitive to its local environment.<sup>14–16</sup> To avoid complications from intramolecular and intermolecular coupling of adjacent O–H bonds, experimentalists have typically studied an isotopic mixture of dilute HOD in  $D_2O$  (Figure 1).<sup>4,17–20</sup> The O–H absorption line shape of such a solution is quite broad ( $260\text{ cm}^{-1}$  fwhm) due to the large distribution of hydrogen-bonding configurations in the liquid. The formation of a hydrogen bond weakens the O–H bond, broadening the proton stretching potential and decreasing its vibrational frequency,  $\omega_{OH}$ . Water molecules participating in strong hydrogen bonds tend to absorb on the low-frequency side of the OH line shape, whereas molecules forming weak or broken hydrogen bonds absorb at higher frequency. By tagging molecules within the absorption line shape with temporally short infrared pulses and then watching how the frequencies of these molecules evolve, we can monitor time-dependent changes in water's hydrogen-bonding structure.

This Account presents the results of recent ultrafast two-dimensional infrared spectroscopy (2D IR) experiments that have provided new information on the stability of different hydrogen-bonding configurations in liquid water.<sup>21–25</sup> A 2D IR spectrum is related to the probability of observing a molecule at given initial and final frequencies after a fixed waiting period. Variation in the vibrational dynamics of spectrally

distinct species has provided new insights into the hydrogen-bonded structure and dynamics of water. These insights are not solely from the experiments but also reflect the parallel development of techniques for calculating 2D IR signals from classical MD simulations.<sup>22,26,27</sup> This allows researchers to turn to simulations to develop an atomistic interpretation of the liquid dynamics that give rise to the measured 2D IR spectra and also provides a test of water models based on their agreement with the experiments. The 2D IR spectroscopy of pure H<sub>2</sub>O forms a separate intriguing story that is not discussed here. In H<sub>2</sub>O, intramolecular and intermolecular coupling between many near-degenerate OH oscillators leads to vibrational excitons that can span up to 12 water molecules depending on hydrogen-bonding configurations and evolve with the fastest motions of the liquid.<sup>24,25,28</sup>

### Frequency–Structure Correlations

In order to interpret the frequency changes measured in 2D IR experiments in terms of the time evolution of water structure, a well-understood connection between  $\omega_{\text{OH}}$  and intermolecular structure is required. It has been known for some time from studies of hydrogen-bonding crystals that a correlation exists between  $\omega_{\text{OH}}$  and  $R_{\text{OO}}$ , the oxygen–oxygen separation between the hydrogen bond donor and acceptor.<sup>29</sup> Modeling of infrared spectroscopy with classical MD simulations using mixed quantum–classical approaches has established the underlying physical origin of this observation. Near-perfect correlation is found between  $\omega_{\text{OH}}$  and the projection of the electric field from all other molecules in the simulation along the O–H bond at the position of the proton (Figure 2A).<sup>16</sup> This can be understood by recognizing that the dominant first-order perturbative correction to the isolated O–H frequency from the liquid resembles a Stark-shift Hamiltonian.<sup>30</sup> Due to its close proximity to the proton, the dominant contribution to the field is from the oxygen of the nearest hydrogen-bonding partner. Changes in the position of the nearest hydrogen-bonding partner relative to the O–H bond induce changes in  $\omega_{\text{OH}}$ .

With a structural description of  $\omega_{\text{OH}}$ , simulations can be used to explore its sensitivity to hydrogen-bonding configuration. Figure 2B shows the correlation between  $R_{\text{OO}}$  and  $\omega_{\text{OH}}$  calculated from second-order perturbation theory.<sup>16,30</sup> Similar correlations have been found for  $\omega_{\text{OH}}$  calculated using other methods.<sup>14,15</sup> At low frequencies ( $\omega_{\text{OH}} \leq 3400 \text{ cm}^{-1}$ ), the correlation is approximately linear, but it widens at higher frequency due to a large distribution of strained or broken hydrogen-bonding geometries. By defining a hydrogen bond using geometric criteria such as  $R_{\text{OO}}$  and the hydrogen-bond-

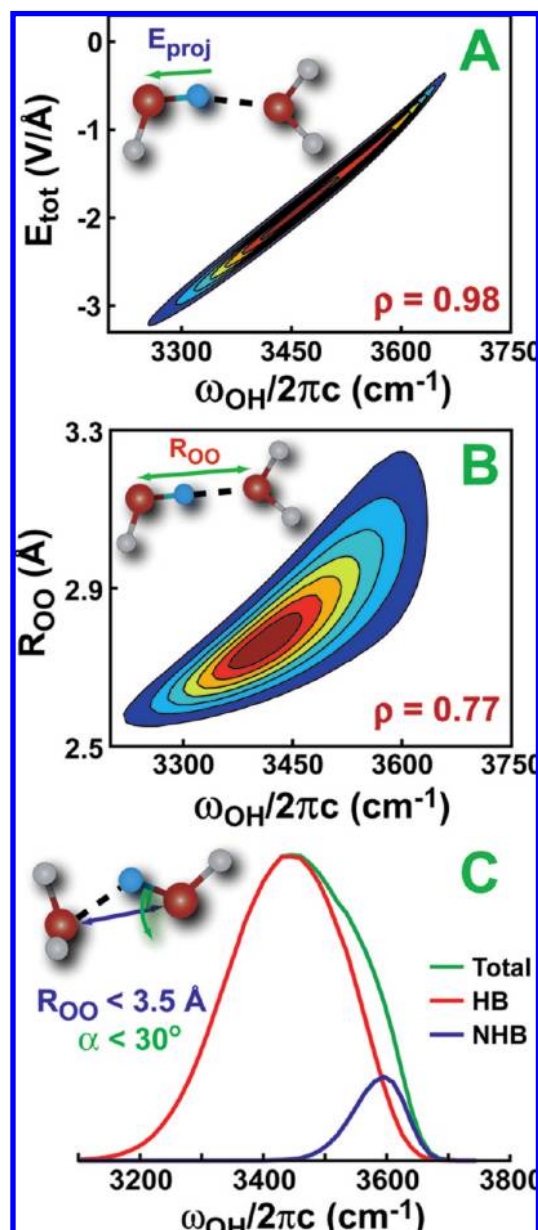


**FIGURE 2.** (A, B) Joint probability distributions of  $\omega_{\text{OH}}$  and geometric order parameters and (C) static frequency distribution for  $\omega_{\text{OH}}$  from MD simulation (green). This distribution is divided into HB (red) and NHB (blue) based on geometric criteria ( $R_{\text{OO}} \leq 3.5 \text{ \AA}$  and HOO angle  $\leq 30^\circ$ ). Adapted from ref 30. Copyright 2005 American Chemical Society.

ing angle (Figure 2C),<sup>13,31</sup> we can divide up the OH frequency distribution into contributions from hydrogen-bonding (HB) and non-hydrogen-bonding configurations (NHB). At any given time,  $\sim 10\%$  of the O–H bonds in the simulation correspond to NHB and absorb preferentially on the high-frequency side of the line shape.

### Scenarios for Hydrogen Bond Exchange

Given that one can distinguish different types of hydrogen-bonding configurations, one can cast questions about water



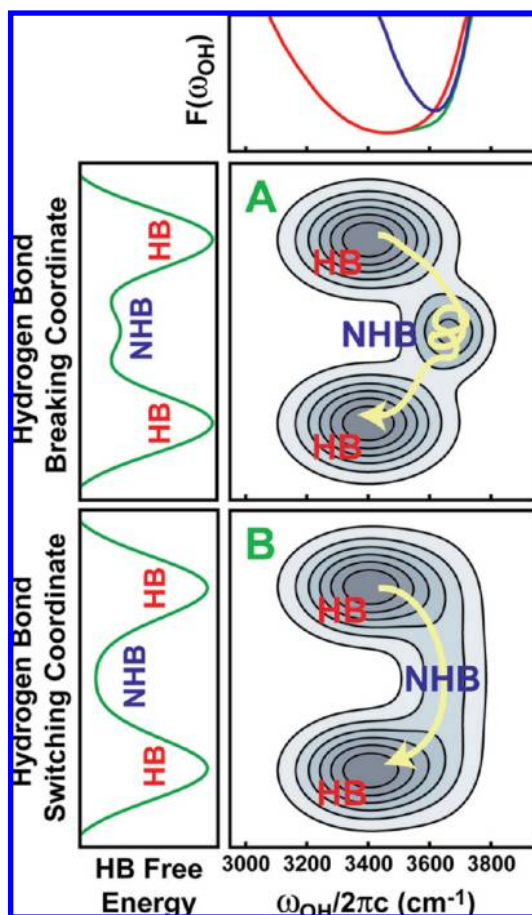


**FIGURE 3.** Cartoon free-energy surfaces describing hydrogen bond exchange for (A) a mixture picture of water and a (B) continuous distribution of structures. In both cases, the free energy along  $\omega_{\text{OH}}$  (above) is the same but the dynamics along this coordinate will differ. Adapted from ref 23. Copyright 2006 American Institute of Physics.

structure in terms of the dynamics by which a hydrogen bond switches from one acceptor to another. Two limiting scenarios, concerted and stepwise processes, are distinguished by their view of NHBs and are pictured through the free-energy surfaces in Figure 3. In a stepwise process a thermal fluctuation ruptures the initial hydrogen bond, but a new acceptor for that bond is not yet available. The entropically stabilized (or dangling) hydrogen bond persists until a later fluctuation presents a new hydrogen bond acceptor. In this picture, also associated with mixture models, HB and NHB occupy stable minima on water's free-energy surface with a barrier  $>kT$  separating them (Figure 3A). An alternative view is that the rearrangement of hydrogen bonds from one acceptor to another happens in one concerted step involving multiple molecules including the HB donor and the initial and final acceptor. Here the NHB configurations are not stable and form a saddle point visited during the course of hydrogen bond exchange (Fig-

ure 3B). In both pictures, the free energy projected along the frequency axis is the same, but qualitatively different dynamics will be observed in  $\omega_{\text{OH}}$ . If NHB configurations form a metastable state, a separation of time scales between the relaxation within both the NHB and HB wells and the exchange between them will be observed. If NHB configurations are unstable, they should return to the HB wells on a time scale of the intermolecular motions of the liquid. Two-dimensional IR measurements can discriminate between these scenarios by tracking how the stretching frequencies of molecules initially in a given configuration change with time.<sup>22,23</sup>

### Frequency-Dependent Dynamics in 2D IR Spectra

Coherent multidimensional spectroscopy has been extensively reviewed, and for the purposes of understanding the present work, we direct attention to those papers that deal with the acquisition and interpretation of 2D line shapes.<sup>32–34</sup> For liquid dynamics, 2D IR provides a mapping of how vibrational excitation at one frequency evolves from an initial set of frequencies to a final set of frequencies. A 2D IR line shape is related to the joint probability of exciting a molecule at an initial frequency,  $\omega_1$  and detecting it at a different frequency  $\omega_3$  after a waiting period  $\tau_2$ . For a vibrational frequency that depends strongly on intermolecular configuration, an inhomogeneous distribution of frequencies is expected. For such a system observed at  $\tau_2 = 0$ , a diagonally elongated line shape appears (Figure 4C) since molecules have not had sufficient time to sample their environments. For longer waiting times, the diagonal 2D IR spectrum becomes symmetric (Figure 4D) as the liquid structure evolves and memory of the initial frequency is lost during  $\tau_2$ . For the anharmonic vibrations studied here, peaks in 2D IR spectra appear as positive/negative doublets. The positive peak corresponds to the ground-state bleach of the  $\nu = 1 \leftarrow 0$  transition whereas the negative peak is due to excited state absorption of the  $\nu = 2 \leftarrow 1$  transition and is anharmonically shifted along  $\omega_3$ .

Figure 5A shows 2D IR spectra for a 1% solution of HOD in  $\text{D}_2\text{O}$  as a function of  $\tau_2$ .<sup>35</sup> At early waiting times, the spectra appear diagonally elongated but broaden as  $\tau_2$  increases, becoming largely homogeneous by 700 fs. The loss of frequency memory in 2D IR lineshapes can be quantified by a number of one-dimensional metrics, including the ellipticity of the line shape,<sup>36</sup> the slope of the nodal line separating the fundamental and overtone transitions,<sup>22,37,38</sup> and the center line slope.<sup>39</sup> Figure 5B displays one of these metrics, the photon echo peak shift<sup>40–42</sup> reconstructed from the 2D data. The double inverse Fourier transform of a diagonally elongated

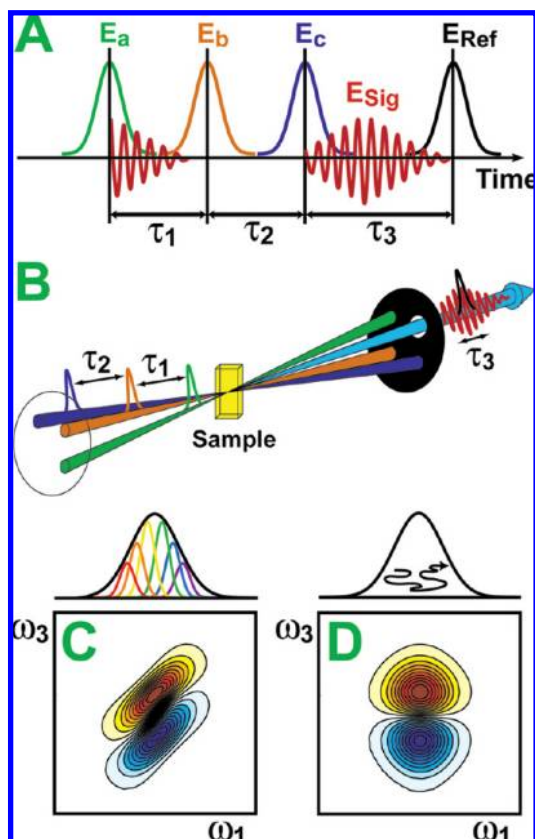


**FIGURE 4.** (A) Pulse sequence and (B) beam geometry used for 2D IR spectroscopy. Three excitation pulses stimulate the emission of a signal field that is detected interferometrically using an external reference field. Fourier transformation of the time delay between the first two excitation pulses ( $\tau_1$ ) and that between the third pulse and the reference ( $\tau_3$ ) yields a 2D spectrum as a function of two frequency axes,  $\omega_1$  and  $\omega_3$ , for a given value of  $\tau_2$ . (C, D) Representative 2D spectra for an inhomogeneous line shape measured with waiting times much shorter and much longer than the correlation time for spectral diffusion.

line shape in the frequency domain yields a similarly diagonally elongated echo in the time domain. At early waiting times, the projection of this echo onto the  $\tau_1$  axis is peaked away from  $\tau_1 = 0$ . The peak shift for a given value of  $\tau_2$  corresponds to the value of  $\tau_1$  that maximizes the integrated photon echo signal and the decay of this quantity describes the average time scale for spectral diffusion of the probed transition. The peak shift calculated from the 2D spectra in Figure 5A shows a sub-100 fs decay, a recurrence near 150 fs due to an underdamped hydrogen bond oscillation, and a slower picosecond decay.

More interesting are the frequency-dependent changes to the 2D spectra with increasing  $\tau_2$ . The  $\tau_2 = 0$  spectrum shows that the high-frequency side of the line shape ( $\omega_{OH} \geq 3500 \text{ cm}^{-1}$ ) is broader along the antidiagonal axis than at low frequency ( $\omega_{OH} \leq 3300 \text{ cm}^{-1}$ ), leading to a pear shape. As  $\tau_2$  increases, the discrepancy in line width between the high- and low-frequency sides becomes more distinct as the blue side of the line shape broadens while at lower frequency it remains compact. If molecules forming strong and weak hydrogen bonds behave similarly, a symmetric line shape should be observed. The asymmetry of the 2D line shape indicates that HB configurations undergo qualitatively different relaxation than NHB ones.

This difference in dynamics can be quantified by examining vertical slices through the 2D spectra.<sup>23</sup> By analogy with hole-burning experiments, such slices correspond to the relaxation of a subensemble prepared at a given frequency, and their time-dependent evolution can be quantified through their first moments (Figure 6). The first moment of slices taken at  $\omega_1 = 3250 \text{ cm}^{-1}$  displays a sharp increase toward band center followed by a pronounced recurrence at 150 fs. This recur-

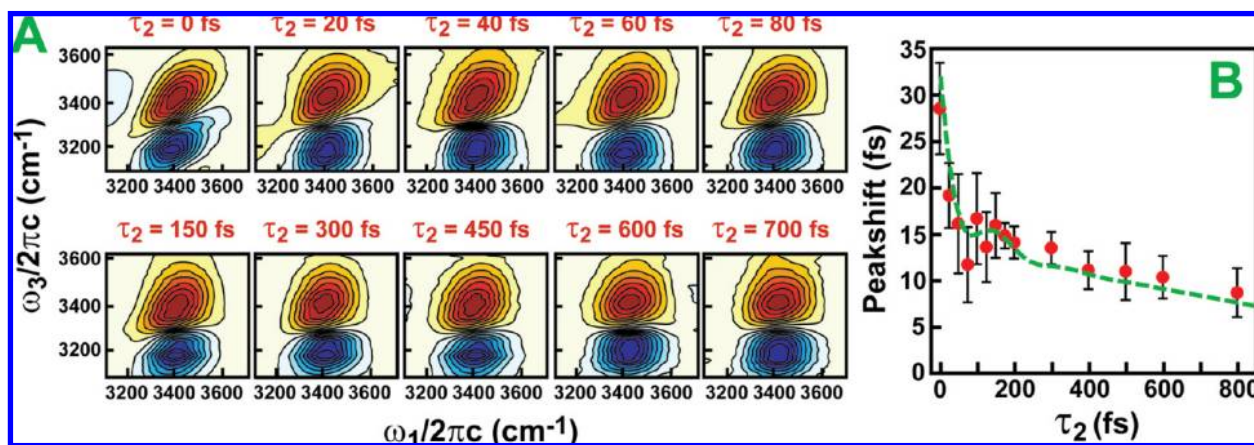


**FIGURE 5.** (A) 2D IR spectra for a  $\sim 1\%$  HOD in  $D_2O$  solution recorded at zzzz polarization as a function of waiting time and (B) the photon echo peak shift calculated from the 2D IR data (red circles) gives the average time scale for spectral diffusion and agrees well with a prediction based on our previously extracted frequency–frequency correlation function (green dashed). Adapted from ref 35. Copyright 2006 American Institute of Physics.



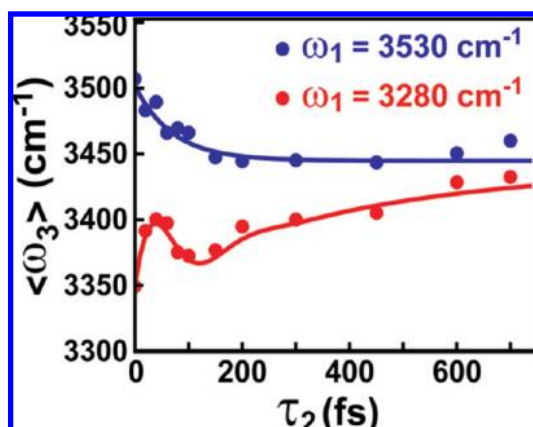


**FIGURE 6.** The first moment of the positive amplitude of slices of the 2D IR spectra for set values of  $\omega_1$ . Adapted from ref 23. Copyright 2006 American Institute of Physics.

rence is indicative of a hydrogen bond oscillation (O–H···O stretch) and indicates that the frequency of hydrogen-bonded oscillators is rapidly modulated as the distance between the proton and the hydrogen-bonding partner changes. At high frequency, no oscillation is observed and the first moment returns to band center within 100 fs. If NHB species are stable, they should persist longer than the time scales for the intermolecular motions of the liquid (~200 fs). Given the time scale and completeness of this decay, NHB configurations do not correspond to stable minima on water's free-energy landscape. Furthermore, the time scale corresponds well with that for librations, implying that reorientational motion plays an important role in hydrogen bond rearrangement.

### Classical Molecular Dynamics Simulations of HOD in D<sub>2</sub>O

MD simulations can be used to determine the molecular origins of the spectral relaxation observed in 2D IR spectra in atomistic detail. Mixed quantum–classical methodologies have been developed for the calculation of multidimensional spectra from classical simulation models. These methods include an empirical system–bath coupling Hamiltonian, which pro-

vides solutions to the Schrödinger equation for the OH potential under the influence of the classical water potential, and mapping methods, which correlate anharmonic vibrational frequencies and transition dipoles from DFT with a collective electrostatic variable that is also available in a classical simulation.<sup>15,26,27</sup> Both methods allow one to obtain long trajectories of OH frequency fluctuations from a classical simulation, which can then be used to calculate observables. Many of these frequency calculation methodologies are readily transferable across different water models, allowing for a direct comparison between these models and experiment.

Schmidt et al.<sup>43</sup> calculated vibrational echo peak shifts for different fixed charge and polarizable water models. The decay of the echo peak shift reflects the average rate of spectral diffusion observed in the 2D IR line shape (Figure 5B). All of the water models examined by Schmidt et al. except polarizable models (FQ) were able to reproduce the hydrogen bond oscillation observed in the echo peak shift experiment<sup>4,16</sup> at early waiting times, yet FQ models more accurately reproduced the long time decay time scale associated with collective rearrangements. Overall, the best agreement with experiment was found for the SPC/E model. Harder et al.<sup>44</sup> also investigated fixed charge and polarizable models, finding reasonable consistency with spectra among fixed charge models and great variation among polarizable models. The best agreement was obtained with the POL5 model, which includes a polarizable dipole out of the plane of the water molecule.

Figure 7 displays 2D IR spectra calculated from an MD simulation employing the SPC/E potential. Vibrational frequencies were calculated using the same method used to produce Figure 2. Calculated line shapes take into account a nonlinear dependence of the O–H stretch transition dipole on  $\omega_{\text{OH}}$ , the non-Condon effect, by making use of an empirically determined relationship between the two quantities.<sup>45</sup> The calculated spectra reproduce the experimentally observed time-dependent asymmetry and center diagonal frequency well but

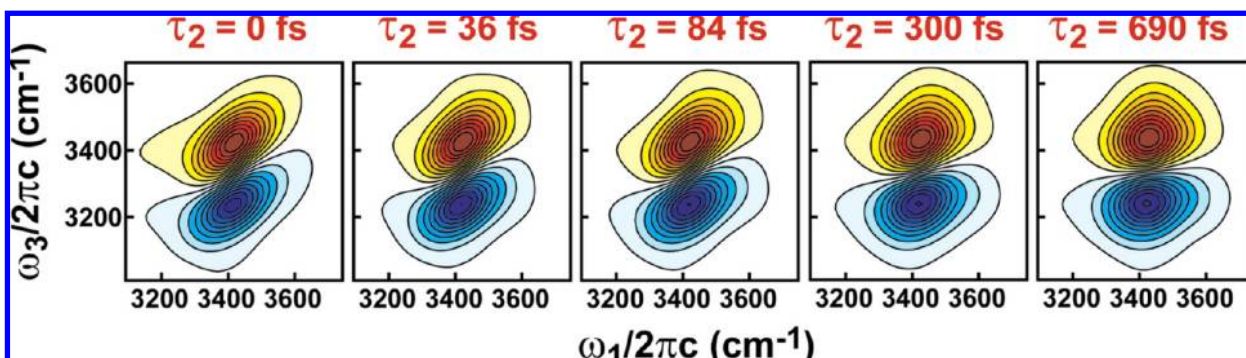


**FIGURE 7.** Calculated 2D IR spectra for the simulation model described in the text. Spectra were calculated for zzzz polarization.

are too narrow along the diagonal axis, indicating that the magnitude of the fluctuations in the simulation may be too small relative to experiment. Nonetheless, the qualitative agreement between the simulation and experiment suggests that we can use classical simulations to directly probe the stability of NHB species.

If NHB configurations correspond to stable minima on water's free-energy surface, then simulated molecules that are in NHB configurations should largely remain in these NHB geometries upon quenching to  $T = 0$  K.<sup>22</sup> Quenching produces "inherent structures" of the liquid that exist at the various minima of its potential energy surface.<sup>5</sup> In simulations, we find that at any given time roughly 7% of molecules have frequencies  $>3600$   $\text{cm}^{-1}$ . Based on the criteria for hydrogen bonding in Figure 3,  $\sim 70\%$  of molecules in this frequency range correspond to NHB configurations. However, upon quenching only 10% of these molecules remain in NHB geometries. If dynamics are run on this NHB subset, most transition to a HB state within 150 fs. On the basis of simulation, stable NHBs appear to be quite rare, comprising  $<0.5\%$  of the configurations found at ambient conditions.

## Reorientation during Hydrogen Bond Exchange

These studies indicate that hydrogen bond switching in water follows a scenario such as that proposed in Figure 3B. Taken together with earlier work, water's first solvation shell largely retains a tetrahedral symmetry and rearrangements are rapid concerted processes. Broken hydrogen bonds form a conduit passed through as a water molecule exchanges hydrogen-bonding partners. However, a proper reaction coordinate for hydrogen bond exchange is not obvious. It is to be expected that rearrangement of hydrogen bonds involves many water molecules, as described through studies of inherent structures.<sup>5</sup> The local motions involved and the relevant length scale over which the motions of water molecules are coupled remains unclear.

The observation that hydrogen bond switching is concerted and that it proceeds on a time scale of librational motion suggests that reorientation of the OH bond is critical for switching. It is reasonable to assume that the transition state for switching would resemble a bifurcated hydrogen bond. These hypotheses can be explored in simulations. A bifurcated transition state suggests that the difference in distance between the lines connecting the hydrogen of the HOD molecule and the two oxygen atoms of the initial and final acceptor,  $\Delta r = R_1 - R_2$ , can serve as a reaction coordinate for hydrogen bond exchange. Figure 8A plots the frequency distribution for mol-

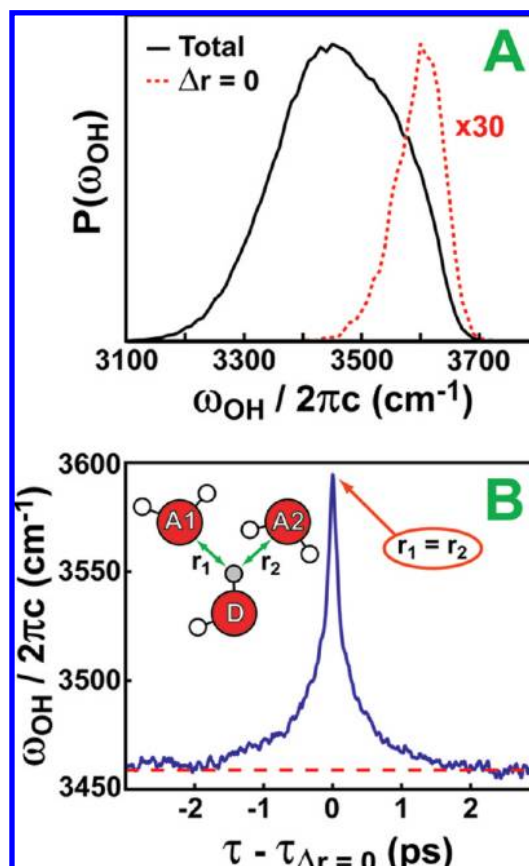


**FIGURE 8.** (A) Frequency distribution of molecules in bifurcated geometries relative to the total frequency distribution and (B) average relaxation behavior of  $\omega_{\text{OH}}$  about HB exchange events. The dashed red line corresponds to the MD value of  $\langle\omega_{\text{OH}}\rangle = 3458$   $\text{cm}^{-1}$ . Adapted from ref 23. Copyright 2006 American Institute of Physics.

ecules with  $\Delta r = 0$ .<sup>23</sup> Compared with the total frequency distribution, molecules in bifurcated geometries are blue-shifted and follow essentially the same frequency distribution as NHB configurations. Figure 8B shows that bifurcated molecules quickly return to frequencies indicative of hydrogen bonds, with time constants of 80 and 500 fs. These time scales correspond to twice the librational period and that for structural rearrangement of the liquid in SPC/E water.<sup>16,23</sup>

Figure 9 shows the free-energy surface calculated as a function of  $\omega_{\text{OH}}$  and  $\Delta r$ . It closely resembles that proposed in Figure 3B. A similar free-energy surface appears in ref 46. The high-frequency side of the line shape serves as a conduit for hydrogen bond exchange, and no stable minimum is observed in the NHB region. Also plotted is a sample trajectory wherein a HOD molecule undergoes underdamped oscillations in the HB region before rapidly moving through the NHB region to form a new hydrogen bond. It should be noted that only 35% of the time that a

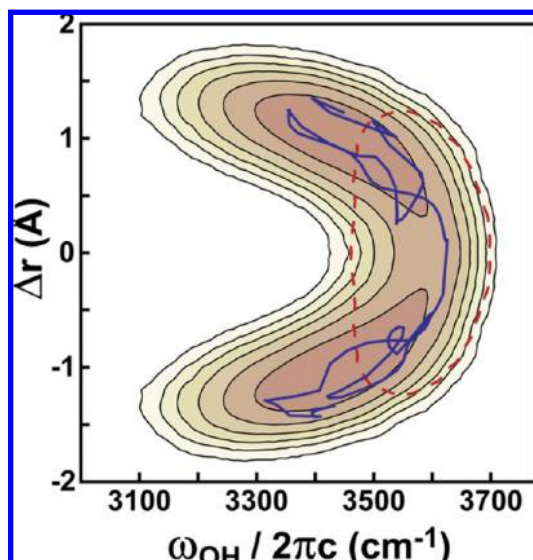


**FIGURE 9.** Free-energy surface for  $\omega_{\text{OH}}$  and the hydrogen bond exchange coordinate,  $\Delta r$ . Black contours correspond to units of  $kT$ . The dashed red contour contains 98% of molecules in NHB configurations, and the blue line is a representative exchange trajectory from MD simulation.

molecule enters the NHB region does it form a new hydrogen bond. A highly blue-shifted frequency is not a unique indicator of the transition state for hydrogen bond exchange.<sup>47</sup> Rather, a blue-shifted frequency can arise from molecules undergoing either exchange or large fluctuations about a stable hydrogen bond, both of which quickly relax back to a hydrogen-bonded state.

A detailed description of the reorientational motion of water molecules in the process of switching has been presented in the recent simulations by Laage and Hynes.<sup>47,48</sup> They suggested that a number of geometric parameters that describe liquid structure undergo large changes concomitant with hydrogen bond exchange. The exchange occurs as a rapid, large angle rotation of the HOD molecule ( $\sim 68^\circ$ ) concurrent with an increase in  $R_{\text{OO}}$  for the original hydrogen bond acceptor and a decrease in  $R_{\text{OO}}$  for the new acceptor. Leading up to the exchange, the original hydrogen bond acceptor becomes overcoordinated and the new hydrogen bond acceptor becomes under-coordinated.

## The Connection between Reorientation and Frequency Shifts

Given the connection between reorientation and hydrogen bond exchange, experiments that probe molecular reorientation, such as pump–probe anisotropy measurements, should display frequency dependence. MD results support this conclusion, showing that the magnitude of the inertial decay time scale in orientational correlation functions is enhanced for molecules initially oscillating at higher fre-

quencies.<sup>14</sup> Experimental attempts to measure frequency dependence of the anisotropy have yielded conflicting results due in part to the differing pump and probe frequencies used as well as a lack of pulses short enough to resolve the inertial decay.<sup>49</sup> Most recently, Moilanen et al.<sup>50</sup> have shown a small frequency dependence to the anisotropy decay,  $r(t) = \langle P_2(\cos \theta(t)) \rangle$ , of the O–D stretch of HOD in H<sub>2</sub>O. Although earlier times were not resolved, by a delay time of 100 fs the anisotropy on the high-frequency side of the O–D absorption line shape has decayed to a lower value than that on the low-frequency side.

In Figure 10, we show additional simulations of orientational correlation functions that remain targets for experimental tests. Figure 10A shows the 2D anisotropy response,  $r = (S_{\parallel} - S_{\perp}) / (S_{\parallel} + 2S_{\perp})$  for the  $\nu = 1 \leftarrow 0$  transition as a function of waiting time. At  $\tau_2 = 0$ , the anisotropy surface uniformly adopts a value of 0.4. However, by  $\tau_2 = 120$  fs, the anisotropy has decayed to a lower value at high frequency along the diagonal axis and in the off-diagonal region, indicating that molecules prepared in NHB states undergo a large degree of reorientation along the course of returning to a hydrogen bond. Slices through this anisotropy for  $\omega_1 = 3300$  and  $3600$   $\text{cm}^{-1}$  are shown in Figure 10B. For molecules that initiate at high frequency, largely NHB configurations, the anisotropy relaxes from 0.4 to a uniform value of 0.25 within 300 fs. For those molecules that manage to return to hydrogen-bonded frequencies within 24 fs as expected in switching, a mean rotation of  $30^\circ$  is necessary. For molecules that initiate from strongly hydrogen-bonded states, little change in anisotropy is observed in the first 300 fs. Only as molecules transition to NHB configurations are significant drops in anisotropy observed.

## Switching through Water Insertion

Although the jump diffusion model put forth by Laage and Hynes<sup>47,48</sup> and the observation of correlated hydrogen bond switching with 2D IR are consistent, we are left with questions about the mechanism for this switching process. In a dense medium such as water, what collective motions give rise to the concerted switching event? If the switching of one hydrogen bond involves at least three molecules, do correlated motions exist between molecules beyond the first or second solvation shell? The minima of the free-energy surface in Figure 9 near  $\Delta r = \pm 1.25$  Å suggests that hydrogen bond switching involves the exchange of water molecules in the first and second solvation shells of the switching molecule, which necessitates the rearrangement of molecules outside of the first solvation shell of the switching molecule.



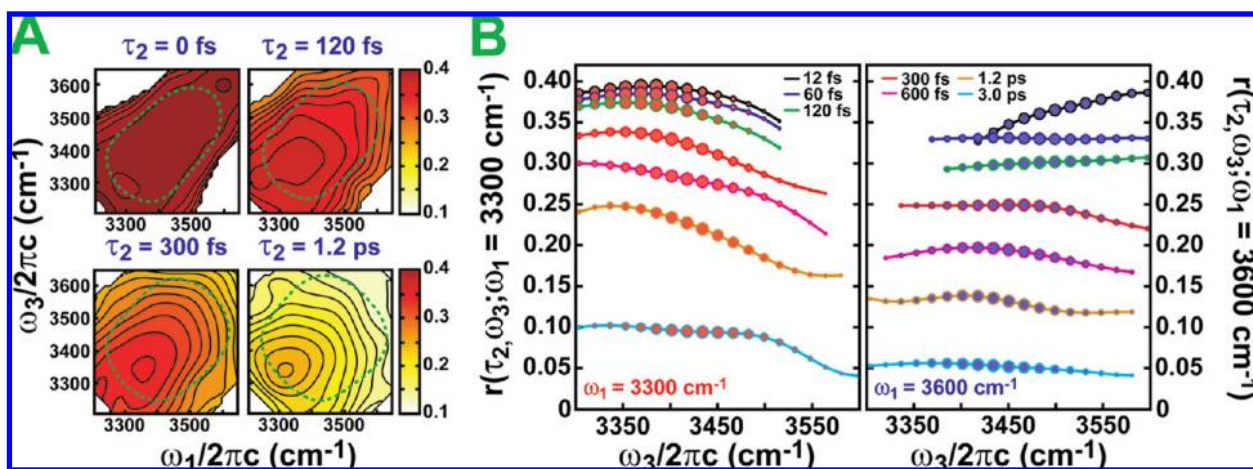


**FIGURE 10.** (A) Calculated 2D IR anisotropy spectra from MD simulation. The dashed green contour on each surface indicates the point where the magic angle response ( $S_{\parallel} + 2S_{\perp}$ ) is equal to 10% of its maximum value. (B) Slices of the calculated spectra for  $\omega_1 = 3300$  and  $3600 \text{ cm}^{-1}$  as a function of  $\tau_2$ . The size of the plotted symbols represent the amplitude of the computed isotropic response for each slice, which tracks how the motionally narrowed population of molecules initially at on the high- and low-frequency sides of the absorption line shape return to band center.

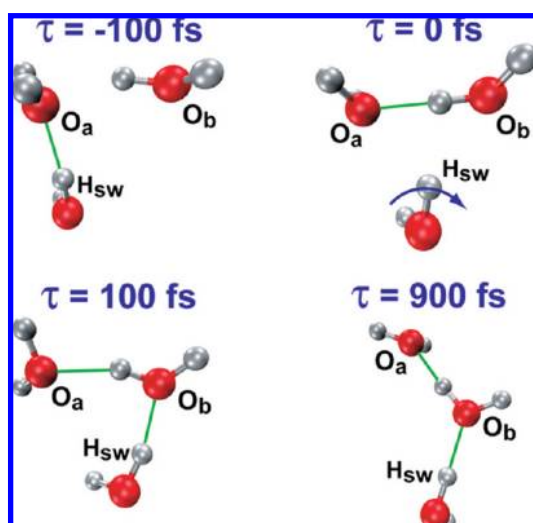


**FIGURE 11.** Snapshots taken from MD simulation over the course of a water insertion event.

One proposal that begins to address these questions is a rearrangement process that involves the insertion of a water molecule from the second solvation shell into a first solvation shell hydrogen bond. Figure 11 shows snapshots from a simulation of SPC/E water that illustrate the course of a hydrogen bond exchange event. The switching hydrogen atom,  $H_{sw}$ , undergoes a large angular rotation that breaks the hydrogen bond between it and  $O_a$ , forming a new hydrogen bond with  $O_b$ . At the bifurcated transition state for the exchange event, one of the hydrogen atoms covalently bonded to  $O_b$  has formed a hydrogen bond to  $O_a$ . If we examine these three water molecules after the switching event, we find that the new hydrogen bond acceptor has inserted across the origi-

nal hydrogen bond formed by  $H_{sw}$  and  $O_a$ . Such an insertion mechanism would provide for concerted rearrangements of multiple molecules in a dense liquid. We observe that in  $\sim 50\%$  of the hydrogen bond exchange events that occur in the MD simulation, a hydrogen bond is formed between the original and new hydrogen bond acceptors, and this suggests that this water insertion mechanism is quite robust. Naturally, microscopic reversibility requires that expulsion of a water molecule from a hydrogen-bonded chain to form a new hydrogen bond will also be present in a roughly equal number of cases.

## Outlook

With its high time resolution and structural sensitivity, ultrafast infrared vibrational spectroscopy has provided a new level of insight into the structural dynamics of liquid water. The combination of experiments and simulation-based modeling allows events along experimentally resolved coordinates to be interpreted with the help of atomistic dynamics, leading to self-consistent descriptions of the underlying reaction dynamics. Two-dimensional IR spectroscopy reveals heterogeneous dynamics and shows that molecules participating in weak or broken hydrogen-bonding geometries quickly reform hydrogen bonds. These results imply that hydrogen-bonding definitions should take into consideration the persistence time of a conformation relative to the intermolecular motions of the liquid, not merely instantaneous geometric criteria. Similar applications of 2D IR to problems of water structure and dynamics are being pursued, including the study of water in

confined environments,<sup>51–53</sup> the study of vibrational energy transfer in water,<sup>24,25,54</sup> the study of aqueous solvation shells,<sup>55</sup> and the study of proton transport in water.<sup>56</sup> At the same time, these results also demonstrate a unique characteristic of 2D IR for the study of chemical reaction dynamics: If a spectral signature of the transition state exists, 2D IR has the ability to serve as a transition-state spectroscopy by following the dynamics of molecules as they leave the transition state and move into either reactant or product channels.

*The authors would like to acknowledge others that played important roles in the experiments and simulations described in this Account: Joel Eaves, Christopher Fecko, Phillip Geissler, Joseph Loparo, Rebecca Nicodemus, and Poul Petersen. We thank the Department of Energy for their long-standing support of this work under Grant DE-FG02-99ER14988, as well as additional support from the Packard Foundation and the ACS Petroleum Research Fund.*

#### BIOGRAPHICAL INFORMATION

**Sean T. Roberts** (B.S. Chemistry, 2003, University of California, Los Angeles) is finishing his doctoral studies at MIT investigating hydrogen bond dynamics and proton transport in water via nonlinear vibrational spectroscopy and computer simulation.

**Krupa Ramasesha** (B.S. Chemistry, 2006, University of Wisconsin, Madison) is pursuing doctoral studies at MIT researching Grotthuss proton transport using 2D IR spectroscopy.

**Andrei Tokmakoff** (B.S. Chemistry, 1989, California State University, Sacramento; Ph.D. Chemistry, 1995, Stanford University) leads a group at MIT that develops experimental methods to study the molecular dynamics of chemical reactions in water and biophysical processes.

#### REFERENCES

- Eisenberg, D.; Kauzmann, W. *The Structure and Properties of Water*; Clarendon Press: Oxford, U.K., 1969.
- Head-Gordon, T.; Hura, G. Water structure from scattering experiments and simulation. *Chem. Rev.* **2002**, *102*, 2651–2670.
- Castner, E. W., Jr.; Chang, Y. J.; Chu, Y. C.; Walrafen, G. E. The intermolecular dynamics of liquid water. *J. Chem. Phys.* **1995**, *102*, 653–659.
- Fecko, C. J.; Loparo, J. J.; Roberts, S. T.; Tokmakoff, A. Local hydrogen bonding dynamics and collective reorganization in water: Ultrafast IR spectroscopy of HOD/D<sub>2</sub>O. *J. Chem. Phys.* **2005**, *122*, 054506.
- Ohmine, I. Liquid water dynamics: Collective motions fluctuation and relaxation. *J. Phys. Chem.* **1995**, *99*, 6767–6776.
- Jimenez, R.; Fleming, G. R.; Kumar, P. V.; Maroncelli, M. Femtosecond solvation dynamics of water. *Nature* **1994**, *369*, 471–473.
- Agmon, N. The Grotthuss mechanism. *Chem. Phys. Lett.* **1995**, *244*, 456–462.
- Soper, A. K. The radial distribution functions of water and ice from 220 to 673 K and at pressures up to 400 MPa. *Chem. Phys.* **2000**, *258*, 121–137.
- Smith, D. W. G.; Powles, J. G. Proton spin-lattice relaxation in liquid water and liquid ammonia. *Mol. Phys.* **1966**, *10*, 451–463.
- Jarzeba, W.; Walker, G. C.; Johnson, A. E.; Kahlow, M. A.; Barbara, P. F. Femtosecond microscopic solvation dynamics of aqueous solutions. *J. Phys. Chem.* **1988**, *92*, 7039–7041.
- Palese, S.; Schilling, L.; Miller, R. J. D.; Staver, P. R.; Lotshaw, W. T. Femtosecond optical Kerr effect studies of water. *J. Phys. Chem.* **1994**, *98*, 6308–6316.
- Fecko, C. J.; Eaves, J. D.; Tokmakoff, A. Isotropic and anisotropic Raman scattering from molecular liquids measured by spatially masked optical Kerr effect spectroscopy. *J. Chem. Phys.* **2002**, *117*, 1139–1154.
- Luzar, A.; Chandler, D. Effect of environment on hydrogen bond dynamics in liquid water. *Phys. Rev. Lett.* **1996**, *76*, 928–931.
- Lawrence, C. P.; Skinner, J. L. Vibrational spectroscopy of HOD in D<sub>2</sub>O III. Spectral diffusion, and hydrogen-bonding and rotational dynamics. *J. Chem. Phys.* **2003**, *118*, 264–272.
- Rey, R.; Moller, K. B.; Hynes, J. T. Hydrogen bond dynamics in water and ultrafast infrared spectroscopy. *J. Phys. Chem. A* **2002**, *106*, 11993–11996.
- Fecko, C. J.; Eaves, J. D.; Loparo, J. J.; Tokmakoff, A.; Geissler, P. L. Ultrafast hydrogen bond dynamics in the infrared spectroscopy of water. *Science* **2003**, *301*, 1698–1702.
- Graener, H.; Seifert, G.; Laubereau, A. New spectroscopy of water using tunable picosecond pulses in the infrared. *Phys. Rev. Lett.* **1991**, *66*, 2092–2095.
- Woutersen, S.; Emmerichs, U.; Nienhuys, H.-K.; Bakker, H. J. Anomalous temperature dependence of vibrational lifetimes in water and ice. *Phys. Rev. Lett.* **1998**, *81*, 1106–1109.
- Gale, G. M.; Gallot, G.; Hache, F.; Lascoux, N.; Bratos, S.; Leicknam, J.-C. Femtosecond dynamics of hydrogen bonds in liquid water: A real time study. *Phys. Rev. Lett.* **1999**, 1068–1071.
- Deak, J. C.; Rhea, S. T.; Iwaki, L. K.; Dlott, D. D. Vibrational energy relaxation and spectral diffusion in water and deuterated water. *J. Phys. Chem. A* **2000**, *104*, 4866–4875.
- Asbury, J. B.; Steinel, T.; Stromberg, C.; Corcelli, S. A.; Lawrence, C. P.; Skinner, J. L.; Fayer, M. D. Water dynamics: Vibrational echo correlation spectroscopy and comparison to molecular dynamics simulations. *J. Phys. Chem. A* **2004**, *108*, 1107–1119.
- Eaves, J. D.; Loparo, J. J.; Fecko, C. J.; Roberts, S. T.; Tokmakoff, A.; Geissler, P. L. Hydrogen bonds in liquid water are broken only fleetingly. *Proc. Natl. Acad. Sci. U.S.A.* **2005**, *102*, 13019–13022.
- Loparo, J. J.; Roberts, S. T.; Tokmakoff, A. Multidimensional infrared spectroscopy of water. II. Hydrogen bond switching dynamics. *J. Chem. Phys.* **2006**, *125*, 194522.
- Cowan, M. L.; Bruner, B. D.; Huse, N.; Dwyer, J. R.; Chugh, B.; Nibbering, E. T. J.; Elsaesser, T.; Miller, R. J. D. Ultrafast memory loss and energy redistribution in the hydrogen bond network of liquid H<sub>2</sub>O. *Nature* **2005**, *434*, 199–202.
- Kraemer, D.; Cowan, M. L.; Paarmann, A.; Huse, N.; Nibbering, E. T. J.; Elsaesser, T.; Miller, R. J. D. Temperature dependence of the two-dimensional infrared spectrum of liquid H<sub>2</sub>O. *Proc. Natl. Acad. Sci. U.S.A.* **2008**, *105*, 437–442.
- Li, S.; Schmidt, J. R.; Corcelli, S. A.; Lawrence, C. P.; Skinner, J. L. Approaches for the calculation of vibrational frequencies in liquids: Comparison to benchmarks for azide/water clusters. *J. Chem. Phys.* **2006**, *124*, 204110.
- Jansen, T. I. C.; Hayashi, T.; Zhuang, W.; Mukamel, S. Stochastic Liouville equations for hydrogen-bonding fluctuations and their signatures in the two-dimensional vibrational spectroscopy of water. *J. Chem. Phys.* **2005**, *123*, 114504.
- Auer, B. M.; Skinner, J. L. IR and Raman spectra of liquid water: Theory and interpretation. *J. Chem. Phys.* **2008**, *128*, 224511.
- Novak, A. In *Structure and Bonding*; Dunitz, J. D., Hemmerich, P., Holm, R. H., Ibers, J. A., Jorgenson, C. K., Neilands, J. B., Reinen, D., Williams, R. J. P., Eds.; Springer-Verlag: New York, 1974; Vol. 18; pp 177–216.
- Eaves, J. D.; Tokmakoff, A.; Geissler, P. Electric field fluctuations drive vibrational dephasing in water. *J. Phys. Chem. A* **2005**, *109*, 9424–9436.
- Kumar, R.; Schmidt, J. R.; Skinner, J. L. Hydrogen bonding definitions and dynamics in liquid water. *J. Chem. Phys.* **2007**, *126*, 204107.
- Jonas, D. M. Two-dimensional femtosecond spectroscopy. *Annu. Rev. Phys. Chem.* **2003**, *54*, 397–424.
- Cho, M. Coherent two-dimensional optical spectroscopy. *Chem. Rev.* **2008**, *108*, 1331–1418.
- Khalil, M.; Demirdoven, N.; Tokmakoff, A. Coherent 2D IR spectroscopy: Molecular structure and dynamics in solution. *J. Phys. Chem. A* **2003**, *107*, 5258–5279.
- Loparo, J. J.; Roberts, S. T.; Tokmakoff, A. Multidimensional infrared spectroscopy of water. I. Vibrational dynamics in 2D lineshapes. *J. Chem. Phys.* **2006**, *125*, 194521.
- Lazonder, K.; Pshenichnikov, M. S.; Wiersma, D. A. Easy interpretation of optical two-dimensional correlation spectra. *Opt. Lett.* **2006**, *31*, 3354–3356.

- 37 Kwac, K.; Cho, M. Two-color pump-probe spectroscopies of two- and three-level systems: 2-Dimensional line shapes and solvation dynamics. *J. Phys. Chem. A* **2003**, *107*, 5903–5912.
- 38 Roberts, S. T.; Loparo, J. J.; Tokmakoff, A. Characterization of spectral diffusion from two-dimensional line shapes. *J. Chem. Phys.* **2006**, *125*, 084502.
- 39 Kwac, K.; Rosenfeld, D. E.; Fayer, M. D. Taking apart the two-dimensional vibrational echo spectra: More information and elimination of distortions. *J. Chem. Phys.* **2008**, *128*, 204505.
- 40 Cho, M.; Yu, J.-Y.; Joo, T.; Nagasawa, Y.; Passino, S. A.; Fleming, G. R. The integrated photon echo and solvation dynamics. *J. Phys. Chem.* **1996**, *100*, 11944–11953.
- 41 de Boeij, W.; Pshenichnikov, M. S.; Wiersma, D. A. On the relation between the echo-peak shift and Brownian oscillator correlation function. *Chem. Phys. Lett.* **1996**, *253*, 53–60.
- 42 Piryatinski, A.; Skinner, J. L. Determining Vibrational Solvation–Correlation Functions from Three-Pulse Infrared Photon Echoes. *J. Phys. Chem. B* **2002**, *106*, 8055–8063.
- 43 Schmidt, J. R.; Roberts, S. T.; Loparo, J. J.; Tokmakoff, A.; Fayer, M. D.; Skinner, J. L. Are water simulation models consistent with steady-state and ultrafast vibrational spectroscopy experiments? *Chem. Phys.* **2007**, *341*, 143–157.
- 44 Harder, E.; Eaves, J. D.; Tokmakoff, A.; Berne, B. J. Polarizable models in the vibrational spectroscopy of water. *Proc. Natl. Acad. Sci. U.S.A.* **2005**, *102*, 11611–11616.
- 45 Loparo, J. J.; Roberts, S. T.; Nicodemus, R. A.; Tokmakoff, A. Variation of the transition dipole moment across the stretching band of water. *Chem. Phys.* **2007**, *341*, 218–229.
- 46 Garrett-Roe, S.; Hamm, P. Three-point frequency fluctuation correlation functions of the OH stretch in liquid water. *J. Chem. Phys.* **2008**, *128*, 104507.
- 47 Laage, D.; Hynes, J. T. On the molecular mechanism of water reorientation. *J. Phys. Chem. B* **2008**, *112*, 14230–14242.
- 48 Laage, D.; Hynes, J. T. A molecular jump mechanism of water reorientation. *Science* **2006**, *311*, 833–835.
- 49 Bakker, H. J.; Rezus, Y. L. A.; Timmer, R. L. A. Molecular reorientation of liquid water studies with femtosecond midinfrared spectroscopy. *J. Phys. Chem. A* **2008**, *112*, 11523–11534.
- 50 Moilanen, D. E.; Fenn, E. E.; Lin, Y.-S.; Skinner, J. L.; Bagchi, B.; Fayer, M. D. Water inertial reorientation: Hydrogen bond strength and the angular potential. *Proc. Natl. Acad. Sci. U.S.A.* **2008**, *105*, 5295–5300.
- 51 Piletic, I. R.; Tan, H.-S.; Fayer, M. D. Dynamics of nanoscopic water: Vibrational echo and infrared pump-probe studies of reverse micelles. *J. Phys. Chem. B* **2005**, *109*, 21273–21284.
- 52 Cringus, D.; Bakulin, A.; Lindner, J.; Vöhringer, P.; Pshenichnikov, M. S.; Wiersma, D. A. Ultrafast energy transfer in water—AOT reverse micelles. *J. Phys. Chem. B* **2007**, *111*, 14193–14207.
- 53 Dokter, A. M.; Woutersen, S.; Bakker, H. J. Inhomogeneous dynamics in confined water nanodroplets. *Proc. Natl. Acad. Sci. U.S.A.* **2006**, *103*, 15355–15358.
- 54 Lindner, J.; Cringus, D.; Pshenichnikov, M. S.; Vöhringer, P. Anharmonic bend-stretch coupling in neat liquid water. *Chem. Phys.* **2007**, *341*, 326–335.
- 55 Park, S.; Fayer, M. D. Hydrogen bond dynamics in aqueous NaBr solutions. *Proc. Natl. Acad. Sci. U.S.A.* **2007**, *104*, 16731–16738.
- 56 Roberts, S. T.; Petersen, P. B.; Ramasesha, K.; Tokmakoff, A.; Ufimtsev, I. S.; Martinez, T. J. Observation of a Zundel-like transition state during proton transfer in aqueous hydroxide solutions. *Proc. Natl. Acad. Sci. U.S.A.*, **2009**, accepted for publication.